15TH IEA HEAT PUMP CONFERENCE
MAY 26–29, 2026 | HOFBURG
VIENNA 2026
DECARBONISATION THROUGH INNOVATION

Test rig and experimental design for a high temperature CO2 pumped thermal energy storage system

Zanil Narsing[a,*], Emily Fricke[a], Silvia Trevisan[a], Rafael Guedez[a], Jan Oledzki[b], Jerémie Lagarde[b], Harry Simpson[b], Alexis Dole[b]

[a]KTH Royal Institute of Technology, Brinellvägen 68, Stockholm, 114 28, Sweden
[b]SynchroStor Ltd., 3 Edgefield Road Industrial Estate, Loanhead Midlothian, EH20 9TB, United Kingdom

Abstract

Decarbonizing the industrial sector is a major challenge facing future energy systems. The industrial sector corresponds to a third of global energy consumption and CO2 emissions. The need to decarbonize this sector of the economy is evident, despite little progress in implementing low carbon technologies. Only 13% of heat was generated with modern renewables in 2022. Heat pumps have been outlined as a key technology in the transition to low-carbon heat sources for their high coefficients of performance. Understanding the benefits of heat pumps on a system level with thermal energy storage, concentrated solar thermal, and an ever-decarbonizing electricity grid is essential to transform the industrial sector. This work includes an overview of a system-level technoeconomic analysis, and the design of the testing facility hosted in the laboratory of KTH's Heat and Power Division. The test rig will validate an R744 (CO2) high temperature heat pump to a TRL 5 by testing different industrial heating and cooling demand profiles. The types of profiles were chosen based on a review of the needs of major industrial subsectors. These include drying, steam, and simultaneous heating and cooling. The operating conditions of the test rig for each demand profile were determined through a combination of heat balances, common heat exchange correlations, and pinch analyses. Finally, this work presents expected operating modes for these profiles along with a preliminary process flow diagram of the test rig.

Keywords: Heat Pump; Pumped Thermal Energy Storage; Industrial Decarbonization; CO2 R744

1. Introduction

The industrial sector corresponds to a third of global energy consumption and a third of global carbon dioxide emissions [1]. The need for heat in the industrial sector of the economy is vast and segmented. One way to divide the industrial heat sector is by temperature levels. One methodology considers low temperature heat demand below 100 °C, medium temperature between 100 and 500 °C, and high temperature greater than 500 °C. In Europe, the low temperature demand typically accounts for 11% of total, non-space heating, industrial heat demand counted via energy per year (TWh/year). Medium temperature demand accounts for 36%. And lastly, high temperature demand accounts for 53% of the demand [2].

All these sectors, but especially medium and high temperature demand levels, must be decarbonized to ensure a scenario within the 1.5 °C increase goal set by the Paris Agreement [3]. Additionally, in the next years, renewable industrial heat demand is expected to increase by 41% from 29.2 EJ in 2022 to 41.1 EJ in 2028. The ambient heat energy captured by heat pumps specifically is forecasted to increase by 36% over these years [2], [4].

Pure electrification of heat may not be the best solution for all countries and all subsectors for a variety of technical, economic, and environmental reasons. Therefore, in the near to medium term, high temperature heat pumps (HTHP) coupled with thermal energy storage present a viable solution to the problem of addressing industrial heat decarbonization.

* Corresponding author. *E-mail address:* zanil@kth.se

As such, many HTHP configurations exist to address these challenges. These different configurations make use of different cycle types (Joule-Brayton or Rankine), different refrigerants (Helium, Argon, CO2/R744, R1234ze, etc.), or different numbers of compressor stages, to name a few. Another big difference in the ecosystem of HTHPs is the end-use goal. Pumped Thermal Energy Storage (PTES) systems present an economically attractive alternative to other long-duration energy storage architecture [5]. The current focus of this subset of Power-to-Heat-to-Power is typically focused on grid connected systems where the benefit of scale helps both economically and technically [6],[7]. However, little attention is paid to the direct-to-user market of high temperature R744 heat pumps coupled with thermal energy storage.

The work of this paper presents the design considerations for a test rig of a high temperature, CO2-based, pumped thermal energy storage system. The goal of the test facility is to validate the heat pump architecture for applicability in direct-to-user industrial heat applications such as food and beverage, pharmaceuticals, and paper.

2. Methodology

2.1. Review of industrial use cases

A review of various industrial heat user demands was conducted prior to determining the operating conditions of the test facility. This was done to ensure the test results would be applicable to the industries which were most likely to adopt this type of PTES system. For the scope of this study, the technical criteria relating to the subsector as a whole weigh heavier than the site-specific economics. A review of the industrial use cases employed in this study is presented in Section 3.

2.2. Cycle design and thermodynamic approach

A set of reverse-Rankine thermodynamic cycles were designed to validate the PTES TRL 5 designation via a custom-built test facility. The facility aims to have target sink temperatures in the range of 200 to 300 °C and a thermal power capacity of 300 kW. The cycles were designed through the basics of a Rankine cycle thermodynamic state point calculation. The specific type of heat pump core which will be used in this study will be a compressor-expander developed by SynchroStor Ltd [6]. A validation of the heat pump operating in both "expander" and "throttling valve" modes will be done. In Figure 1, the state points for both modes can be seen. An isentropic efficiency of 90% is assumed for the compression and expansion phases of the heat pump. During the experimental campaign, this is a parameter to test and verify.

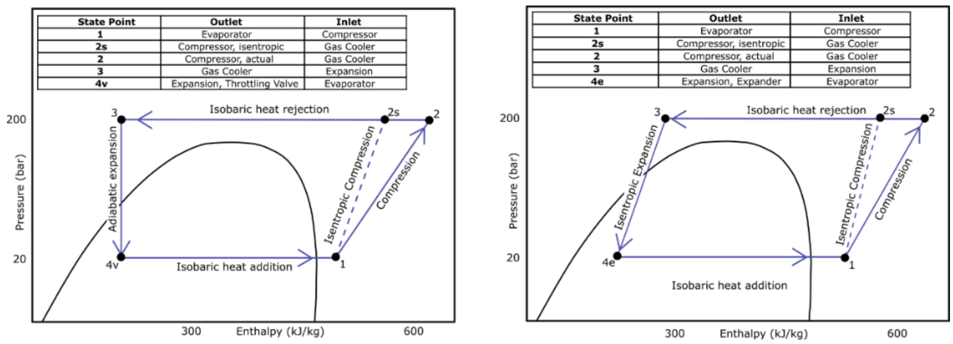

Figure 1. State Points for a Reverse-Ranking Cycle using a Throttling Valve (left) and Expander (right)

The governing equation for determining the energy balance is based on a change in enthalpy and mass flow rate, as seen in Eq. (1).

$$\dot{Q} = \dot{m} \cdot \Delta H \tag{1}$$

2.3. Determination of component specifications

The test rig for this project will be installed at the KTH Heat and Power Division (HPT) laboratory. Source and sink cycles have been developed and will be installed to supply and extract heat, respectively, from the central heat pump gas cycle. The major components to determine at this stage of development are the evaporator and gas cooler heat exchangers, sink cycle and source cycle pumps, source cycle heater, and thermal energy storage capacities. Due to a variety of limiting factors, the compressor power has been limited to about 100 kW of electrical input. This limitation then affects the mass flow rates and thermal power generation possible, effectively creating the boundary conditions needed to specify the major equipment needed to design the laboratory rig. This process is described in the following subsections.

2.3.1. Heat exchangers

The thermophysical properties of R744 lead to many opportunities and challenges related to heat transfer. Due to the relatively low critical point of CO2, approximately 31 °C and 73.8 bar, heat rejection typically occurs transcritically. This has benefits such as decoupling the gas cooler pressure and the saturation pressure. The optimal gas cooler pressure is therefore dictated by outlet temperature and refrigerant charge [7]. The downside is that when operating near the critical point, the density and heat capacity of the refrigerant vary dramatically, leading to uneven heat transfer in the heat exchanger. When compared to other common refrigerants, R744 has a lower compression ratio, leading to higher isentropic efficiencies and a high volumetric efficiency.

Another benefit of operating in the transcritical range of R744 is the high temperature yield of the sink fluid. Since there is no phase change in the transcritical region, there is a high temperature glide of both the R744 and the sink fluid. With proper heat exchanger design, the R744 can be cooled to within a few degrees of the incoming sink fluid [7].

2.3.1.1. Evaporator

A heat balance between the source fluid and R744 was used as the basis for calculating the outlet temperature of the source fluid. The inlet temperature of the source fluid was considered as an input variable which is controllable in the test sequence. The governing heat equations are Eq. (2) and Eq. (3). For the initial estimation of sizing for the heat exchangers, no thermal losses to the atmosphere were considered. Therefore, to satisfy the heat balance, the power transmitted to the refrigerant, R744, is equal to the heat transferred from the source fluid.

$$\dot{Q}_{source} = \dot{m}_{source} c_p \Delta T \tag{2}$$

$$\dot{Q}_{R744} = \dot{m}_{R744} \Delta H \tag{3}$$

$$\dot{Q}_{R744} = \dot{Q}_{source} \tag{4}$$

$$T_{outlet} = T_{inlet} + \frac{\dot{m}_{R744} \Delta H}{\dot{m}_{source} c_p} \tag{5}$$

The specific heat capacity of the source fluid is determined at the bulk average temperature of the fluid through the heat exchanger. This reliance on the outlet temperature requires that this equation be solved iteratively. An initial guess of the outlet temperature is made and updated until a convergence criterion is reached. Eq. (5) can then be modified to the Eq. (6).

$$(T_{outlet})' = T_{inlet} + \frac{\dot{m}_{R744} \Delta H}{\dot{m}_{source} \cdot c_p(T_{outlet})} \tag{6}$$

Once the outlet temperature of the source side fluid is calculated, the sizing of the heat exchanger can take place since all four of the temperatures are known. As seen in Figure 2, a thermal circuit is used to characterize the heat exchange process.

$$\dot{Q} = UA \cdot LMTD \tag{7}$$

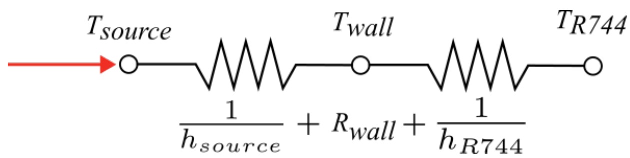

Figure 2. Heat Exchanger Simplified Thermal Circuit

An estimation of the heat exchange area is determined based on the thermal circuit. The total thermal resistance can be found using Eq. (8). Total thermal resistance can also be found by adding each resistive element, seen in Eq. (9). The heat exchange area can therefore be found by Eq. (10).

$$R_{Total} = \frac{LMTD}{\dot{Q}_{evap}} \left[\frac{K}{W}\right] \tag{8}$$

$$R"_{Total} = \frac{1}{h_{source}} + R"_{wall} + \frac{1}{h_{R744}} \left[\frac{K}{Wm^2}\right] \tag{9}$$

$$A_{HX} = \frac{R_{Total}}{R"_{Total}} [m^2] \tag{10}$$

An estimate of the wall contact resistance, R_{wall}, can be found from existing literature. The heat transfer coefficients, h_{source}, and h_{R744}, can be calculated based on the method from [8]. For this sizing exercise, a counterflow tube-in-tube heat exchanger configuration is modelled. The Reynolds number and Prandtl number for the two fluids must be calculated. For flow in a circular pipe, the Reynolds and Prandtl number can be found using Eq. (11) and Eq. (12). The heat transfer coefficient can then be found by calculating the Nusselt number using the Dittus-Boelter equation, Eq. (13). For this approximation, hydrodynamically and thermally fully developed, turbulent flow in a smooth circular pipe is assumed [8]. Where n in Eq. (13) is either 0.4 if the fluid is being heated, or 0.3 if the fluid is being cooled. In the case of the evaporator, the Nusselt number calculation of the R744 refrigerant uses 0.4 because it is being heated (gaining energy) and the Nusselt number calculation of the source fluid uses 0.3 because it is being cooled (losing energy).

$$Re = \frac{4\dot{m}}{\pi D_h \mu} \tag{11}$$

$$Pr = \frac{c_p \mu}{k} \tag{12}$$

$$Nu = 0.023 \cdot Re^{4/5} \cdot Pr^n \tag{13}$$

$$h = \frac{Nu \cdot k}{D_h} \left[\frac{W}{m^2 K}\right] \tag{14}$$

2.3.1.2. Gas cooler

The other major heat exchanger considered in the design process of this test rig is the gas cooler. The gas cooler is responsible for delivering heat to the sink fluid while extracting heat from the refrigerant. The process for calculating the conditions of the gas cooler is the same as for the evaporator, and follows the method outlined in the previous section.

2.3.1.3. Pinch analysis

A pinch analysis was conducted to estimate the required flow rates for the sink and source circuits. The pinch analysis plots temperature as a function of the heat exchanged between the two fluids. To do so, the temperature for each fluid at each normalized power-step must be calculated.

In both the gas cooler and evaporator heat exchangers, the R744 temperature steps can be calculated based on a change in enthalpy, Eq. (15). Since the heat rejection or addition are modelled as isobaric, the R744 temperature can be found using thermophysical properties.

$$H_{R,i+1} = H_{R,i} - \frac{d\dot{Q}}{\dot{m}_{R744}} \tag{15}$$

The thermal oil design condition for the sink circuit does not change phase. Therefore, the temperature steps for the pinch analysis can be calculated using Eq. (16). It is important to note that the specific heat (c_p) of the sink fluid is a function of temperature, and therefore, the specific heat needs to be determined at each time step. This is done via lookup tables using thermophysical properties provided by manufacturers.

For the evaporator, as the name suggests, the refrigerant undergoes a phase change. The method of calculating the refrigerant temperature steps based on a change in enthalpy still applies, however, the temperature will not change for sections of the heat exchanger which have been determined to exist within vapor dome. The methodology for calculating the source temperature steps is similar to that of the sink. The source temperature change can be calculated using Eq. (17).

$$T_{sink,i+1} = T_{sink,i} - \frac{d\dot{Q}_{gas\ cooler}}{\dot{m}_{sink} \cdot c_{p,sink}} \tag{16}$$

$$T_{source,i+1} = T_{source,i} - \frac{d\dot{Q}_{evaporator}}{\dot{m}_{source} \cdot c_{p,source}} \tag{17}$$

The pinch temperature can then be found by a difference between the two interacting fluids, Eq. (18) and Eq. (19). By using the equations presented above, the mass flow rates of the sink and source fluids can be adjusted based on a target pinch temperature. An iterative process is used because of the dependency of the thermophysical properties on temperature for both the sink and source fluids.

$$T_{pinch,evaporator} = min(T_{source} - T_{R744}) \tag{18}$$

$$T_{pinch,gas\ cooler} = min(T_{R744} - T_{sink}) \tag{19}$$

2.3.2. Thermal energy storage tanks

The initial sizing of the thermal energy storage tanks follows a simple heat balance model. Selecting the desired hours of storage allows the necessary size to be calculated. The efficiency term, η, is used to represent the efficiency of the heat exchange process between the fluid and the thermal energy storage.

$$\dot{Q}_{TES} = \eta \cdot \dot{Q}_{fluid} \tag{20}$$

2.3.3. Auxiliary heaters and coolers

Since this test rig will be in the KTH HPT laboratory, it must simulate the heat demand and waste heat systems of an industrial facility. Therefore, a set of heaters and coolers will be installed in the sink and source loops to simulate and control these facets.

The source loop will require a heater, which will simulate the waste heat stream from industry. The maximum power required by this heater will be equal to that of the evaporator. As heat is transferred to the refrigerant, this same amount of heat is then required to be put back into the source fluid to ensure steady state operation. Thus, the source heater regulates the source fluid inlet temperature to the evaporator.

The sink loop will require a sink cooler, which, in a similar manner to that of the source loop, is needed to regulate the inlet temperature to the gas cooler heat exchanger and balance the heat rejection with heat injection to ensure steady state operation.

3. Industrial Heat Use Case Review

Different industrial sectors use heat in different ways. It is important to match the demand of the industry to the low-carbon technology. A benefit of R744 as a refrigerant is its high temperature glide during compression. Aiming to make use of this benefit, certain industries are targeted as stakeholders in this project. This section will describe a few industries which are compatible with this type of heat pump.

3.1. High temperature drying

Drying is the removal of liquid from raw or processed materials. The liquid is typically water but can also be other types of solvents. The end-product is classified as either dehydrated, with a water content of less than 2.5% dry basis, or dried, with a water content of greater than 2.5% dry basis [9]. The drying process adds value to the product in different ways, such as through product recovery and isolation, reduction of mass and volume for transportation and storage, creation of powders and dyestuffs, and food preservation. Although drying historically has been used mainly in the food and beverage industry, today the use case for drying spans many different industries such as pharmaceuticals, chemicals, and bioenergy [10]. There are many different types of drying, however, the form which will be discussed here is spray drying due to its temperature applicability and broad sector matching.

Spray drying is a method to produce powders from a liquid or slurry by rapidly drying with a hot gas [10]. The gas is typically air, and at a temperature of between 150-200 °C. The process is rapid, typically on the order of 30 seconds or less, and the particle size is small, typically between 10 and 200 μm. The process is known for being high quality and inexpensive when compared to freeze drying on a cost per kilogram of water removed basis. Common products used in spray drying include milk powders, whey powder, dry cream, infant formula, flavorings, cereal, and coffee. For the pharmaceutical industry, it is used to produce antibiotics, additives, and medical ingredients. The industrial sector uses spray drying to produce catalysts, paint pigments, and ceramic materials [10]. Table 1 shows typical temperature ranges seen in spray drying applications.

High temperature CO2 heat pumps would be a good technology fit for spray drying applications because of the high temperature glide needed for the air. Another benefit of R744 heat pumps is the ability to produce the required temperature glide in a single stage, allowing for a more compact design of equipment.

Table 1. Spray drying applications and typical temperature ranges [10]

Process	Temperature (°C)
Whey and Milk Powders	150-300
Coffee	270
Fertilisers	200-400
Extruded Feed	100-175
Charcoal Briquettes	130-170

3.2. Steam

Steam is a common heat transfer mechanism for many industries throughout the world. In Europe, steam accounts for about 40% of the useful energy demand in the industrial sector, with it taking the majority of the demand in the chemical, paper, and food sectors [11]. The type and quality of the steam depend on the applications, but many industries use 10 bar gauge (barg) steam. At this pressure, the steam has a temperature of 184 °C. For the sake of building a boundary condition for steam, an assumed superheating and subcooling of 10 K can be considered and will produce the following parameters in Table 2.

The steam industry can be addressed by high temperature CO2 heat pumps, as will be shown in following sections. However, a high degree of superheating is required to meet the steam quality requirements of many industries. Additionally, a high degree of enthalpy will remain in the refrigerant after heat rejection, and therefore, to achieve a high COP, industries which require both steam and hot water should be targeted. A heat pump system with an expander is also recommended to recapture as much energy as possible.

Table 2. Steam at 10barg parameters with 10K superheat and 10K subcooling

Parameter	Value
Steam Pressure	10 barg
Saturation Temperature	184 °C
Superheated steam temperature	194 °C
Condensate Temperature	174 °C
Source Inlet Temperature	40 °C
Source Outlet Temperature	15 °C

3.3. Heating and cooling

The food and beverage industry has many different subsectors which use both heating and cooling in their processes. Some examples include the dairy industry using heat for pasteurization and cooling for storage, distilleries using heating for evaporation and cooling for condensation and storage, and breweries for wort boiling and cooling. The dairy industry in particular has many subsets for which different levels of heating and cooling are needed. These are summarized below in Table 3 [12].

Industries requiring both heating and cooling are a good match for CO2 heat pumps because of the thermophysical properties of R744. The evaporation temperatures are aligned with the needs of cooling industries, in the range of 5 to -20 degrees Celsius. The heat rejection in the gas cooler can simultaneously provide heat up to 215 °C with a pressure ratio of 10. An analysis of these state points can be seen further in this document.

Table 3. Process temperature ranges of selected dairy products [12]

Process	Temperature (°C)
Fresh Product Storage	0-5
Ice cream, etc.	< -20
Pasteurisation	70-100
Sterilisation/UHT	115-150
Cheese Production	50-65
Drying (milk, whey)	150-300

4. Results and Discussion

4.1. Experimental campaign and cycle design

Five heat pump cycles have been developed to match with expected real-world demands. The rig in the lab will have a water/glycol mixture as the source fluid and thermal oil for the sink fluid. These were selected based on applicability, flexibility, cost, and availability. However, the industrial sector is broad and employs many types of sink and source fluids. Therefore, careful consideration was paid to have an operable lab-scale test facility, while also generating data which can be used to validate up to TRL 5 the applicability of this heat pump for larger industries. Each of the cycles will be described in the following subsections. The results of their component modelling and cycle design will also be shown in a summary at the end.

4.1.1. Spray drying, expansion

The first cycle is based on the application of spray drying. As mentioned, spray drying is an especially interesting case for R744 heat pumps because of the high degree of sink temperature glide. In an industrial setting, air will need to be lifted from 20-40 °C to 200-400 °C [13], [14] to effectively create powders. The heat pump will be in “expansion” mode, meaning that some of the energy remaining in the refrigerant after passing through the gas cooler will be transferred to the motor shaft via a controlled expansion in the expansion cylinder.

Refer to Table 4 for a summary of all key cycle input parameters. With the current operating states, the COP of the gas cycle will be 3.17. The results of the pinch analysis can be seen in Figure 3. The results of the model with a target pinch temperature of 10 K were that a mass flow rate of 0.65 kg/s of refrigerant and a volume flow rate of 3.14 m^3/hr and 1.88 m^3/hr for the sink and source fluids, respectively is required. The targeted thermal power delivery for this cycle is 190 kW.

A simulation of a pinch analysis using air as the sink fluid can be seen in Figure 4. The simulated air system will be able to generate dry air at 200 °C, and a flow rate of 1.1 kg/s. Table 5 shows the results of the KPIs for this cycle design.

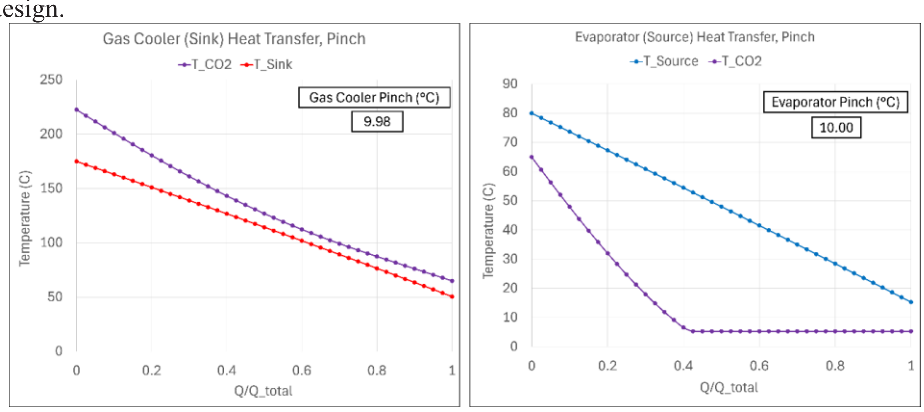

Figure 3. Gas Cooler (left) and Evaporator (right) Pinch Analysis Results for the Spray Drying with Expansion case. A mass flow rate of 0.65 kg/s of refrigerant and a volume flow rate of 3.14 m^3/hr and 1.88 m^3/hr for the sink and source fluids, respectively is required to achieve a pinch temperature of 10 K.

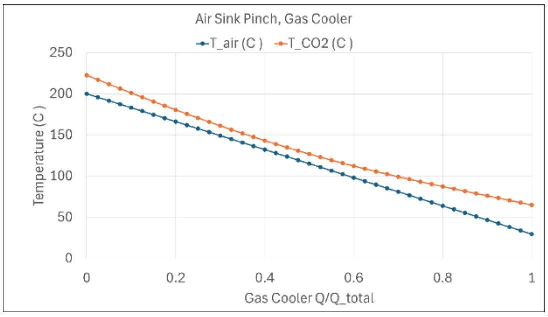

Figure 4. Simulated Pinch Analysis of Dry Air for the Spray Drying, Expansion case

4.1.2. Spray drying, throttling valve

The second case, spray drying with throttling valve is similar to the previous case. The targeted thermal power for this case is 170 kW, slightly less than that of the expansion case. Using the same method, a mass flow rate of refrigerant will be 0.54 kg/s. The sink and source fluids will have volumetric flow rates of 2.67 and 1.72 m^3/hr, respectively.

4.1.3. Steam, expansion

The steam case only considers expansion because of the high amount of remaining energy after the gas cooling phase. Because steam must change phase from liquid water to saturated steam, the refrigerant must reach a much higher delivery temperature for there to be a reasonable pinch difference. This cycle reaches the highest refrigerant temperature and highest sink outlet temperature of all the cases, of 235 °C and 225 °C, respectively. The results of the pinch analysis can be seen in Figure 5. A target thermal power delivery of 202 kW will require a refrigerant mass flow of 1.15 kg/s. The volumetric mass flow rates of the sink and source fluids are 2.86 m^3/hr and 1.51 m^3/hr, respectively.

The simulated air sink fluid pinch analysis can be seen in Figure 6. With the expected refrigerant max temperature of 235 °C, a simulated steam generation of 10 barg, 200 °C, and 0.04 kg/s can be calculated. The COP of this system, 2.82, considers the use of the entirety of the gas cooling capacity, meaning the process has use of hot water generation too, not only steam.

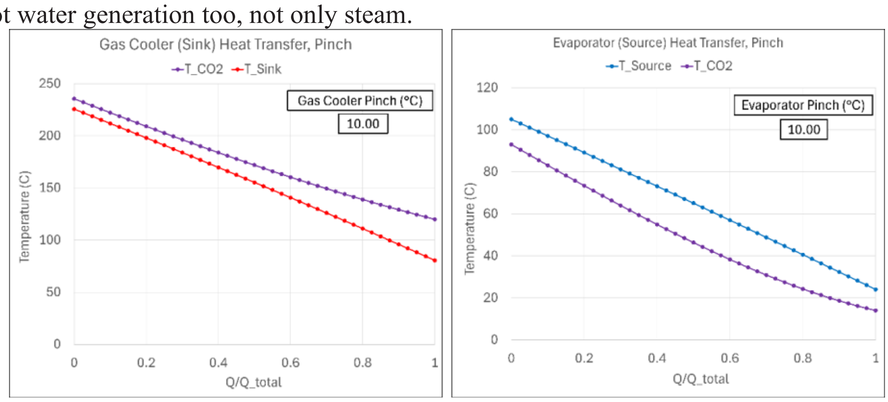

Figure 5. Gas Cooler (left) and Evaporator (right) Pinch Analysis Results for the Steam with Expansion case. A mass flow rate of 1.15 kg/s of refrigerant and a volume flow rate of 2.86 m^3/hr and 1.51 m^3/hr for the sink and source fluids, respectively is required to achieve a pinch temperature of 10 K.

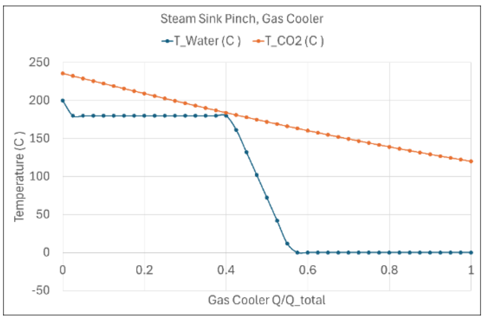

Figure 6. Simulated Pinch Analysis of Steam with Expansion

4.1.4. Heating and cooling, expansion

Many industrial subsectors have a need for simultaneous heating and cooling, and therefore, cycles to demonstrate the R744 heat pump's capability has been created. There is additional benefit to having this generation from a single unit, as opposed to multiple systems throughout the facility. The heating and cooling cycles also make use of the special piston-based compressor mechanics, allowing for a pressure ratio of 10 within a single stage, taking the R744 from 19.5 bar to 195 bar.

Industrial facilities needing both heating and cooling frequently use thermal oil and water/glycol as the heat transfer fluids, so no additional simulated sink or source was analyzed. The result of the pinch analysis for the heating and cooling with expansion case can be seen in Figure 7. The target thermal power delivered is 175 kW.

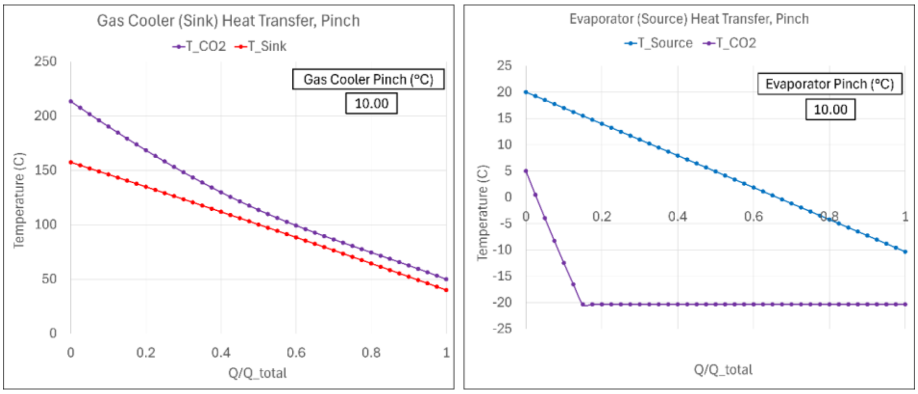

Figure 7. Gas Cooler (left) and Evaporator (right) pinch analysis results for the heating and cooling with expansion case. A mass flow rate of 0.55 kg/s of refrigerant and a volume flow rate of 3.16 m^3/hr and 3.34 m^3/hr for the sink and source fluids, respectively is required to achieve a pinch temperature of 10 K.

4.1.5. Heating and cooling, throttling valve

To test the difference in performance between the throttling valve and the expander, the same input parameters are used between the heating and cooling throttling valve case and the heating and cooling expander case.

4.1.6. Cycle input summary

Table 4. Input Parameter Summary for Cycle Design

Parameter	*Unit*	Drying with Expansion	Drying with Throttling Valve	Steam with Expansion	Heating and Cooling with Expansion	Heating and Cooling with Throttling Valve
Evaporator Pressure	*bar*	40	40	49	19.5	19.5
Gas Cooler Pressure	*bar*	200	200	200	195	195
Compressor Inlet Temperature	*C*	65	65	93	5	5
Expansion Inlet Temperature	*C*	65	55	120	50	50
R744 Mass Flow Rate	*kg/s*	0.65	0.54	1.15	0.55	0.55
Heat Pump Thermal Power Delivery	*kW*	190	170	202	175	175
Source Inlet Temperature	*C*	80	80	105	20	20
Source Pressure	*bar*	1.01	1.01	1.01	1.01	1.01
Source Volume Flow Rate	*m^3/hr*	1.88	1.72	1.51	3.34	3.34
Sink Inlet Temperature	*C*	50	40	80	40	40
Sink Pressure	*bar*	1.01	1.01	1.01	1.01	1.01
Sink Volume Flow Rate	*m^3/hr*	3.14	2.67	2.86	3.16	3.16

4.1.7. Cycle performance summary

The Key Performance Indicators (KPI) for the cycle design can be seen below in Table 5. These include the Coefficient of Performance (COP), the targeted thermal power delivered, the Pressure Ratio (PR), the refrigerant temperature lift, and the sink outlet temperature. These indicators were used to ensure that the heat pump cycles simulated would align with the industrial use cases presented.

Table 5. Cycle Performance KPIs Summary

Parameter	Unit	Drying with Expansion	Drying with Throttling Valve	Steam with Expansion	Heating and Cooling with Expansion	Heating and Cooling with Throttling Valve
COP	-	3.2	2.7	2.8	2.6	2.1
Heat Pump Thermal Power	kW	190	170	202	175	175
Pressure Ratio	-	5.0	5.0	4.1	10.0	10.0
Refrigerant Temperature Lift	C	157.5	157.5	142.6	208.5	208.5
Sink Outlet Temperature	C	174.9	173.8	225.7	157.5	157.5

4.2. Component sizing and boundary conditions

In Table 6, Table 7, Table 8, and Table 9, the boundary conditions of the sink cycle pump, source cycle pump, evaporator heat exchanger, and gas cooler heat exchanger, respectively, are presented. These boundary conditions are the results of modelling based on the five validation thermodynamic cycles presented in Section 4.1.

Table 6. Sink Cycle Pump Boundary Conditions

Parameter Boundary Condition	Min	Max
Volumetric Flow Rate (m^3/hr)	2.7	3.2
Temperature (°C)	15	80
Pump Outlet Pressure Required (bar)	1.82	1.95
Pump Head (m)	21.5	22.9

Table 7. Source Cycle Pump Boundary Conditions

Parameter Boundary Condition	Min	Max
Volumetric Flow Rate (m^3/hr)	1.5	3.3
Temperature (°C)	-10	105
Pump Outlet Pressure Required (bar)	1.21	1.31
Pump Head (m)	12.1	12.7

Table 8. Evaporator Heat Exchanger Boundary Conditions

Parameter Boundary Condition	Min	Max
R744 Inlet Temperature (°C)	-20.3	14.1
R744 Outlet Temperature (°C)	5	93
R744 Pressure (bar)	19.5	49
R744 Mass Flow Rate (kg/s)	0.54	1.15
Source Fluid Inlet Temperature (°C)	20	105
Source Fluid Outlet Temperature (°C)	-10	26
Source Fluid Mass Flow Rate (kg/s)	0.4	1.0
Evaporator Duty (kW)	108	130.5

Table 9. Gas Cooler Heat Exchanger Boundary Conditions

Parameter Boundary Condition	Min	Max
R744 Inlet Temperature (°C)	213.5	235.7
R744 Outlet Temperature (°C)	50	120
R744 Pressure (bar)	195	200
R744 Mass Flow Rate (kg/s)	0.54	1.15
Sink Fluid Inlet Temperature (°C)	40	80
Sink Fluid Outlet Temperature (°C)	157.5	225.7
Sink Fluid Mass Flow Rate (kg/s)	0.6	0.8
Gas Cooler Duty (kW)	170	202

Following the methodology from section 2.3.3, the thermal energy storage tanks will have a target capacity of about 45 minutes of discharge time, based on a thermal mass of 200 kg and 100 kg for the hot TES and cold TES, respectively. The source fluid heater and sink fluid cooler require 127 kW and 202 kW of thermal capacity to ensure steady state operation.

4.3. Process flow diagram and system overview

The process flow diagram (PFD) of the system can be seen in Figure 8. The PFD details the three main circuits of the arrangement. The source circuit is the loop on the bottom of the PFD, containing the source pump, evaporator, source heater, and the cold TES unit. The sink circuit is the loop on the top of the PFD, containing the sink pump, gas cooler, hot TES unit, sink cooler, and sink heater. In the center of the PFD is the heat pump gas loop charged with R744 refrigerant. An additional coolant oil loop is connected to the compressor-expander machine.

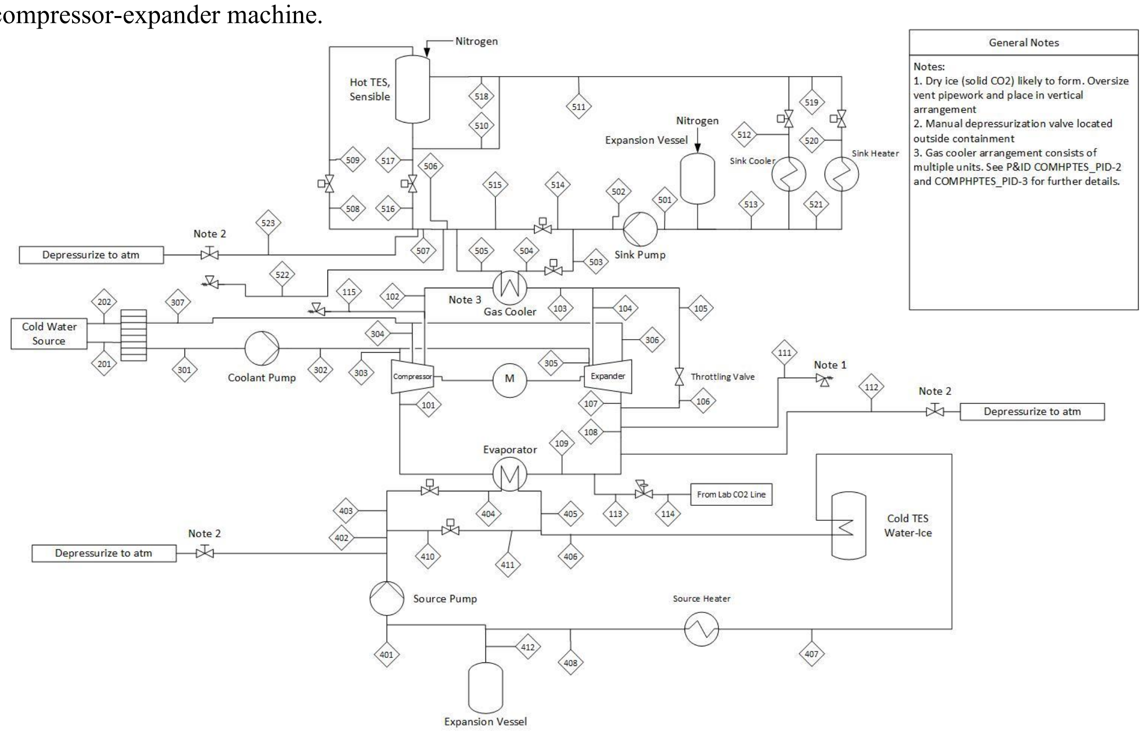

Figure 8. Process flow diagram (PFD) for the heat pump testing facility to be installed at the KTH Heat and Power Division Laboratory

5. Conclusion and Future Work

In this paper, an introduction to the need for industrial heat decarbonization was presented and a focus on the knowledge gap in direct-to-user PTES systems was established. To address this gap, an experimental campaign will be conducted to validate a heat pump PTES system designed to operate according to the thermal demands of various industrial subsectors. These subsectors were described using their preferred heat transfer fluid and temperature ranges which can be achieved by the R744 compressor-expander heat pump. Then, based on the requirements of these industries, a set of five thermodynamic reverse-Rankine cycles were developed and described. The design steps and methodology were then presented to illustrate the pre-engineering work needed to construct the test rig at the KTH Department of Heat and Power Technology in Stockholm, Sweden. As a result, the boundary conditions of the major components, such as heat exchangers, pumps, and thermal energy storage tanks, were presented based on the requirements of the thermodynamic cycle design. Lastly, an initial process flow diagram was shown to illustrate how the three major cycles are interconnected.

The next steps for this project are to finalize the thermal energy storage tank configuration and begin the procurement phase. A set of modelling efforts are also planned to coincide with the experimental campaign. These include a techno-economic modelling study to understand the best use of R744 heat pumps, with particular focus on demand matching and dispatch optimization. Different technical configurations will be tested in this techno-economic work, such as the benefit of expansion mode on this heat pump. Additionally, a dynamic model of the test rig itself will be created to characterize the heat transfer phenomena expected during testing.

Acknowledgements

This research was funded by the CETPartnership, the Clean Energy Transition Partnership under the 2023 joint call for research proposals, co-funded by the European Commission (GA N°101069750) and with the funding organizations detailed on http://cetpartnership.eu/funding-agencies-and-call-modules .

References

[1] IRENA, “Industry,” Industry. Accessed: Feb. 28, 2025. [Online]. Available: https://www.irena.org/Energy-Transition/Technology/Industry

[2] “Mapping and analyses of the current and future (2020 - 2030) heating/cooling fuel deployment (fossil/renewables) - European Commission.” Accessed: May 13, 2025. [Online]. Available: https://energy.ec.europa.eu/publications/mapping-and-analyses-current-and-future-2020-2030-heatingcooling-fuel-deployment-fossilrenewables-1_en

[3] “The Paris Agreement | UNFCCC.” Accessed: Nov. 12, 2025. [Online]. Available: https://unfccc.int/process-and-meetings/the-paris-agreement

[4] “Heat – Renewables 2023 – Analysis,” IEA. Accessed: Feb. 28, 2025. [Online]. Available: https://www.iea.org/reports/renewables-2023/heat

[5] A. M. Rabi, J. Radulovic, and J. M. Buick, “Pumped Thermal Energy Storage Technology (PTES): Review,” *Thermo*, vol. 3, no. 3, pp. 396–411, Jul. 2023, doi: 10.3390/thermo3030024.

[6] “SynchroStor.” Accessed: Jul. 09, 2025. [Online]. Available: https://www.synchrostor.co.uk/

[7] X. Zhang and H. Yamaguchi, *Transcritical CO2 Heat Pump: Fundamentals and Applications. Chapter High Temperature CO2 Heat Pump System and Optimization*, 1st ed. Wiley, 2021. doi: 10.1002/9781118380055.

[8] F. P. Incropera, D. P. DeWitt, T. L. Bergman, and A. S. Lavine, Eds., *Fundamentals of Heat and Mass Transfer Seventh Edition*, 7. ed., International student version. Hoboken, NJ: Wiley, 2013.

[9] H. Vega-Mercado, M. Marcela Góngora-Nieto, and G. V. Barbosa-Cánovas, “Advances in dehydration of foods,” *J. Food Eng.*, vol. 49, no. 4, pp. 271–289, Sep. 2001, doi: 10.1016/S0260-8774(00)00224-7.

[10] J. M. Domínguez, “2.51 - Drying,” in *Comprehensive Biotechnology (Second Edition)*, M. Moo-Young, Ed., Burlington: Academic Press, 2011, pp. 727–735. doi: 10.1016/B978-0-08-088504-9.00129-X.

[11] S. Madeddu *et al.*, “The CO2 reduction potential for the European industry via direct electrification of heat supply (power-to-heat),” *Environ. Res. Lett.*, vol. 15, no. 12, p. 124004, Nov. 2020, doi: 10.1088/1748-9326/abbd02.

[12] “MILK AND WHEY POWDER | Dairy Processing Handbook.” Accessed: Jul. 01, 2025. [Online]. Available: http://dairyprocessinghandbook.tetrapak.com/chapter/milk-and-whey-powder

[13] D. Velić, M. Bilić, S. Tomas, and M. Planinić, “Simulation, calculation and possibilities of energy saving in spray drying process,” *Appl. Therm. Eng.*, vol. 23, no. 16, pp. 2119–2131, Nov. 2003, doi: 10.1016/S1359-4311(03)00165-0.

[14] Ö. Ö. Taner, “Energy and production analysis of a dairy milk factory: A case of study,” *J. Therm. Eng.*, vol. 9, no. 5, Art. no. 5, Oct. 2023, doi: 10.18186/thermal.1370731.